Original Article

Journal of Tissue Engineering
Volume 8: 1–11

DOI: 10.1177/2041731416686532
journals.sagepub.com/home/tej
SAGE

A clinically relevant in vivo model for the assessment of scaffold efficacy in abdominal wall reconstruction

Jeffrey CY Chan[1,2], Krishna Burugapalli[3], Yi-Shiang Huang[2], John L Kelly[1,2] and Abhay Pandit[2]

Abstract

An animal model that allows for assessment of the degree of stretching or contraction of the implant area and the in vivo degradation properties of biological meshes is required to evaluate their performance in vivo. Adult New Zealand rabbits underwent full thickness subtotal unilateral rectus abdominis muscle excision and were reconstructed with the non-biodegradable Peri-Guard®, Prolene® or biodegradable Surgisis® meshes. Following 8 weeks of recovery, the anterior abdominal wall tissue samples were collected for measurement of the implant dimensions. The Peri-Guard and Prolene meshes showed a slight and obvious shrinkage, respectively, whereas the Surgisis mesh showed stretching, resulting in hernia formation. Surgisis meshes showed in vivo biodegradation and increased collagen formation. This surgical rabbit model for abdominal wall defects is advantageous for evaluating the in vivo behaviour of surgical meshes. Implant area stretching and shrinkage were detected corresponding to mesh properties, and histological analysis and stereological methods supported these findings.

Keywords

Animal model, abdominal wall reconstruction, biologic meshes, dimensional measurement, quantitative stereological analysis

Date received: 15 September 2016; accepted: 7 December 2016

Introduction

Hernia repair remains one of the most frequently performed surgical procedures worldwide. It is estimated that approximately 10%–20% of midline laparotomy incisions will develop incisional hernia. The recurrence rate after primary repair of ventral hernia and incisional hernia ranged from 25%–54%.[1–5] The recurrence rate increased further after a second repair.[6] Incisional hernia occurs in 19% of morbidly obese patients without previous hernia undergoing gastric bypass procedure, but this increased to 40% in those with a previous hernia.[7] In one study with long-term follow up, the recurrence rate after primary repair was above 60% versus over 30% for mesh repair.[8]

The conventional synthetic polymers such as nylon,[9,10] polyethylene,[11] polypropylene,[12–18] polytetrafluoroethylene (PFTE),[19–24] and polyethylene terephthalate (PET)[25] have been widely applied in hernia repair surgery for more than 50 years. The recently introduced biological meshes, composed mainly of extracellular matrix components, are designed to undergo in vivo degradation and implant area remodelling to replace the deficient tissues.[26,27]

[1]Department of Plastic, Reconstructive and Hand Surgery, University Hospital Galway, Galway, Ireland
[2]CÚRAM–Centre for Research in Medical Devices, National University of Ireland Galway, Galway, Ireland
[3]Biomedical Engineering Theme, Institute of Environment, Health and Societies, Brunel University London, Uxbridge, UK

Corresponding author:
Abhay Pandit, CÚRAM–Centre for Research in Medical Devices, National University of Ireland Galway, Galway, Ireland.
Email: abhay.pandit@nuigalway.ie

Background

To assess the repair of the abdominal wall, in vivo models are commonly used to evaluate the tissue response and mechanical performance of surgical meshes. In a typical abdominal wall defect model, a standardized defect size is pre-determined and created on the abdominal wall of the animals.[28,29] A defect of the abdominal wall is usually created by excising the abdominal wall tissues, whether in the midline position or lateral positions, usually by standardizing the size removed. Meshes are then implanted and the abdominal wall is assessed for mechanical failure and tissue response.

Implanted meshes, in particular the degradable/biologic meshes, can stretch considerably with or without hernia formation. Both clinical scenarios may contribute to abdominal wall laxity and weakness.[30–32] Similarly, shrinkage/contraction seen with non-degradable synthetic meshes[33,34] does not produce abdominal weakness or herniation, and hence – for this limited interpretation, could dubiously be regarded as a successful repair. However, mesh contraction has been associated with many of the clinical complaints associated with unsatisfactory clinical results, including chronic pain and abdominal stiffness, without abdominal wall herniation.[35,36]

The design and approach of these current in vivo abdominal wall defect models have obvious limitations. First, the defects created are not clearly defined anatomically. A defect of the abdominal wall is usually created by excising the abdominal wall musculature, whether in the midline position or lateral positions, usually by standardizing the size removed, but not the excision anatomy. Second, current in vivo models make no attempt to adjust for animal growth and the possible influence this might have on the implant area. Therefore, any changes in the implant area that might occur will not be confidently distinguished, whether it is related to animal growth or effects of the implant/scaffold itself. Third, there could be animal-to-animal variations in normal growth. Thus, a model with methodology to control for animal growth is desired. An intra-animal control is needed.

The pre-determined abdominal defect size fails to consider the anatomical structure, which leads to undefined anatomical excision and an inability to distinguish the implanted area. In addition, the animal-to-animal variation in animal growth is unaccounted for. Therefore, an animal model that could control for this variation is desired. Finally, in the case of an idealized regenerative biologic implant, the anatomy would theoretically be restored (or partially restored), leaving behind a smaller defect. Hence, it is crucial to control for such changes, to distinguish whether a residual defect is due to true regeneration of tissues or due to animal growth around the unrestored defect (erroneously attributed to ‘regeneration’).

Aims

Herein, we have developed a reproducible in vivo rabbit hernia model that allows for the detection of commonly established abdominal wall repair outcomes, including wound healing complications, hernia formation, seroma formation, intraperitoneal adhesions, fistula and dehiscence of graft–tissue interface to facilitate an objective evaluation of biological meshes. In this study, we have established a rabbit model based on abdominal tissue domain loss, by creating surgical defects focussed on anatomical boundaries with an internal control to optimize the in vivo evaluation of the efficacy of biological meshes to promote reconstruction of the abdominal wall.

Materials and methods

Animals

In this study, 15 young adult New Zealand white rabbits (weight: 3.0–3.5 kg) were utilized. Experiments were conducted with approval from the National University of Ireland, Animal Ethics Committee. A license was obtained from the Department of Health and Children, Dublin, Ireland, as required by the Cruelty of Animals Act (1876). Certificate B (no. B100/3685) approved the study design.

Experimental groups

According to the mesh types, a total of 15 rabbits were divided into 3 groups with 5 animals in each. Three model implants were chosen to repair the abdominal wall to test the relevance of the in vivo model. In order to stimulate implant site contraction, a heavy-weight polypropylene mesh (Prolene; Ethicon Endo-Surgery Inc., USA) was chosen. Single-layer, degradable, small intestinal submucosa (Surgisis; Cook Medical Inc., USA) was chosen to stimulate implant site stretching. A highly cross-linked bovine pericardium Peri-Guard (Synovis Surgical Innovations) implant was chosen as a control/model implant that was expected to be unchanged in size at the end of the study period.

Experimental and surgical procedures

The surgical technique used in this study is illustrated in Figure 1.

Animals were acclimatized for at least 1 week to the local environment before surgery. Hairs were removed from the anterior abdominal wall with electric hair clippers. Induction of anaesthesia was carried out with intramuscular Ketamine (35 mg/kg) and Xylazine (5 mg/kg). An isoflurane and oxygen gas mixture was used for maintenance of anaesthesia. A midline incision was performed through the skin and subcutaneous fat. The rectus abdominis muscle was exposed on

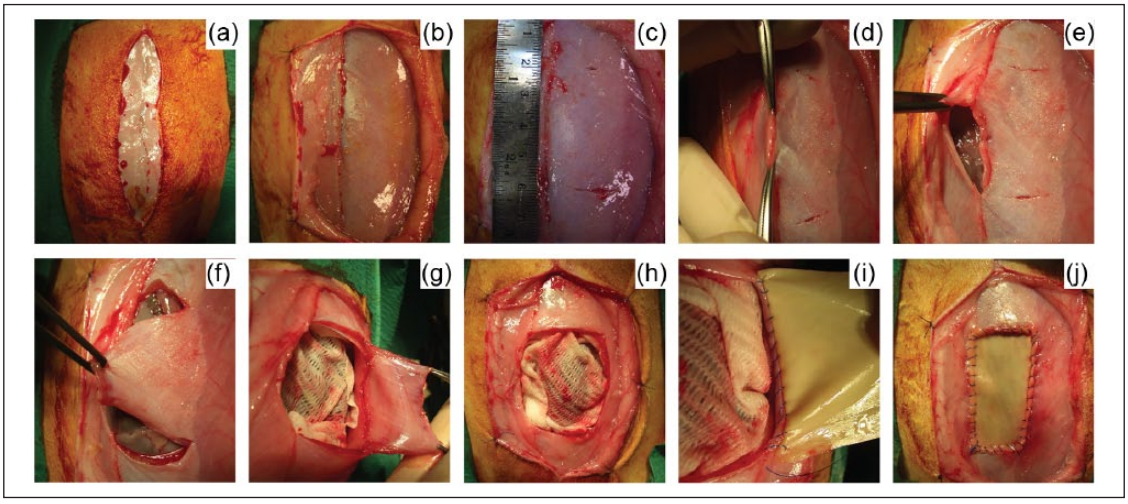

Figure 1. Illustration of the surgical technique used in this study: (a) midline abdominal skin incision, (b) exposure of the left rectus abdominis muscle, (c) marking of a 4-cm length on the left rectus abdominis muscle, (d) haemostats used to lift the abdominal wall away from organs to prevent inadvertent injury, (e) entry into the peritoneal cavity, (f) excision of left rectus muscle performed on medial, superior and inferior aspects, (g) lateral edge of rectus muscle marked. Moist swab left in the peritoneal cavity to prevent trauma to organs, (h) left rectus abdominis muscle excised, (i) repair/replacement with Peri-Guard implant using 4/0 polypropylene suture and (j) repair completed with Peri-Guard implant.

the left side. Excision of the rectus abdominis muscle was performed unilaterally on the left side including the peritoneal layer. A 4-cm-longitudinal length was marked on the mid-portion of the rectus abdominis muscle. Excision was carried out for this longitudinal length (4 cm) along the borders of the linea alba and the linea semilunaris (width). The resultant abdominal wall defect (the excised mid-portion of the rectus abdominis muscle of 4 cm length) was repaired with a similar sized implant (like for like, 'replacement') using a running 4/0 polypropylene suture. Each rabbit was randomized to receive Prolene, Peri-Guard or Surgisis. Each rabbit was given a standard dose of prophylactic antibiotic Enrofloxacin (5 mg/kg) subcutaneously and analgesia butorphanol (0.25–0.4 mg/kg) was administered subcutaneously for 48 h post surgery. The rabbits were maintained in a controlled environment in cages until sacrifice. All rabbits were observed regularly for wound complications (including infection, bleeding and dehiscence) and the occurrence of herniation, seroma and mesh/implant extrusion. Minor herniation was closely observed until the end of the study period. After 56 days, the rabbits were euthanised with 2 mL of sodium pentobarbital (Dolethal) under anaesthesia. The anterior abdominal wall tissues were removed with care to preserve bilateral rectus abdominis muscles and the surrounding tissues. The implant area was identified by the presence of polypropylene sutures used for securing the implant at the time of repair. The presence of adhesions was noted. The size of the wounds was traced using tracing paper, and photographs were taken as required. The implant areas were then cut and preserved in 4% neutral buffered formalin for histological analysis.

Evaluation of implant contraction/stretching

Following euthanasia, the anterior abdominal wall of each rabbit was harvested for analysis. The implant areas were recorded with tracing paper. The corresponding adjacent right rectus abdominis muscle of each rabbit was also traced. These tracings were scanned to obtain a digital image. The area of the implants and their corresponding right rectus abdominis muscles were determined using ImageJ software (v1.43). The percentage contraction or stretching of the area, width or length of the implant area was evaluated using the following formula

$$\text{Percentage change} = \frac{[(\text{Implant left side}) - (\text{Control right side})]}{(\text{Control right side})} \times 100\%$$

Histological analysis

Formalin-fixed tissues of the implant area were dehydrated through a series of graded ethyl alcohol solutions (50%, 75%, 95% and 100%), cleared with xylene and embedded in paraffin using an automatic tissue processor (Leica ASP 300; Leica Microsystems, Germany). Paraffin sections of 5 µm thick were stained with Masson's Trichrome stain. The stained sections were observed under light microscope, and digital images were captured for qualitative histomorphology and quantitative stereological analysis (BX51 microscope, DP-70 digital camera; Olympus Europe, Germany).

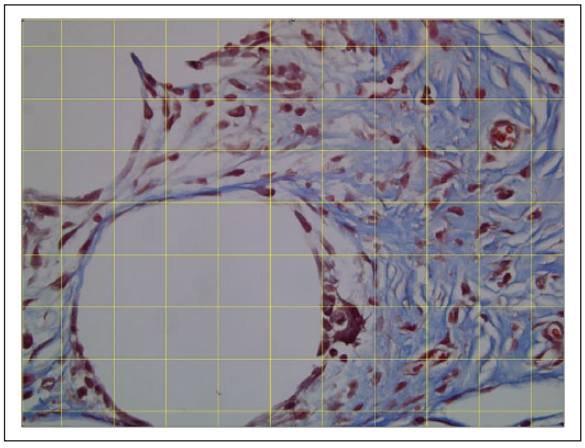

Figure 2. Stereological quantification using a standard grid of $33 \times 33\ \mu m^2$ with a total of 80 intersections at 400X image magnification. This grid is transposed on the implant area from a Prolene mesh repair group. Intersection points on the grid that correspond to the points of interest (cell nuclei, fibroblast, collagen or implant) were counted and the volume fraction of each parameter was calculated.

Quantitative stereological analysis

The stereological methods used for the quantitative analysis of tissue response and degradation parameters in this study were based on work previously reported.[37,38] Briefly, the stereological approach is based on sampling, and sampling needs to be isotropic. Since the abdominal wall is an anisotropic layered structure, its stratified nature required the use of a vertical uniform random sampling method to obtain isotropy in the vertical sections. At least six non-overlapping random fields of view per section per stereological parameter, six sections per scaffold and five scaffolds per group per time point were used for adequate sampling of the implant area. The test systems (counting grids/cycloids) provided by an image analysis software (ImageJ; National Institutes of Health, USA) were used to enable the counting of points for stereological analysis. The stereological parameters used for the quantification of histology sections included volume fraction (V_v) of cell nuclei, V_v of fibroblasts, V_v of blood vessels, V_v of the implant, and V_v of new host collagen. These were estimated using a standard grid made of $33 \times 33\ \mu m^2$ with a total of 80 intersections on 400X image magnification. An example of the standard grid is shown in Figure 2. V_v of each parameter was determined using the formula

$$\left[V_v = \frac{P_p}{P_T} \right]$$

where P_p is the number of points of the parameter of interest and P_T is the total number of points.

Statistical analysis

Statistical analyses were carried out using statistical software InStat (version 3.1a; GraphPad Software Inc., USA). For the implant area, width and length, the Gaussian distribution of the data was assessed using the Kolmogorov and Smirnov test. The difference in variances was tested using the Bartlett test. As the data passed these tests, statistical difference between groups was analysed by one-way analysis of variance (ANOVA). Tukey's honestly significant difference test was used for post hoc evaluation of differences between groups. A p-value of <0.05 was considered to be statistically significant. All data represented are expressed as mean ± standard error (SE) of mean.

Results

Macroscopic appearance

All animals tolerated the procedure well, and there was no wound-healing complication observed in the study groups. Figure 3 demonstrates the representative examples of the scaffolds after 8 weeks of recovery.

In the Surgisis group, the implants were found to stretch significantly at 8 weeks as expected. Mature fibrous collagenous tissues mixed with fragile granulation tissues were observed in this area. Blood vessels could be seen on the surface of the implant site. Although there was host tissue ingrowth in place of the implant, these were too weak to support the abdominal wall.

Hence, hernia formed in all cases repaired with the Surgisis implant within 4 weeks. In the Prolene group, external observations showed that skin and subcutaneous tissue overlying the implant area was tethered to the underlying implant. When observed from the peritoneal side, the meshes were contracted which occasionally distorted the implant area, resulting in stiffening of the abdominal wall. Mainly tough fibrous collagenous tissue was observed over the non-degradable implant. Adhesions were also present. Host tissue had grown into the interstices of the polypropylene mesh. This tissue reaction resulted in an almost rigid, inflexible implant area. Blood vessels were observed on the surface of the implants, but these were less prominent when compared to the Surgisis and Peri-Guard groups. In the Peri-Guard group, the implant showed a degree of contraction or wrinkling of the implant. Only a thin layer of collagenous tissue was present over the implant on the peritoneal side. Additionally, a small number of blood vessels were seen traversing the surface of the implant. The implant appeared to be less securely integrated to the overlying subcutaneous tissue, especially where the implant wrinkling was observed.

Implant dimension measurements

The percentage change in area, width and length of the implants is presented in Figure 4.

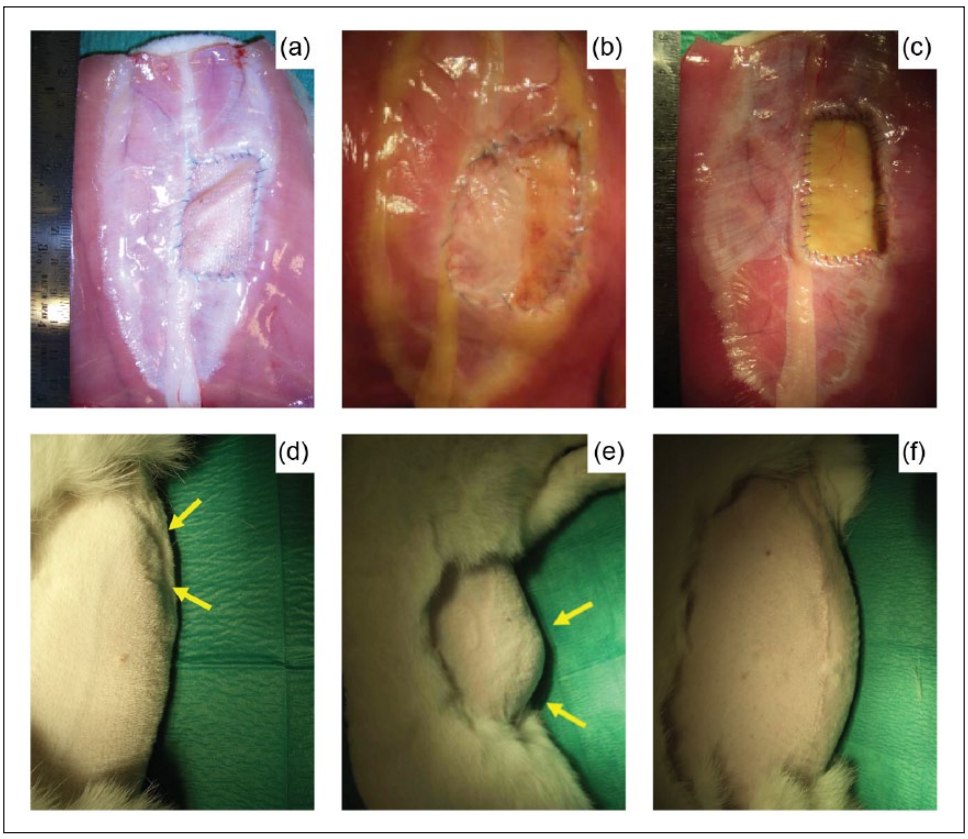

Figure 3. Explants after 56 days showing the peritoneal surface of (a) Prolene, (b) Surgisis implant and (c) Peri-Guard implant. In vivo rabbit model showing (d) abdominal wall repair with Prolene showing slight contour deficit due to mesh shrinkage, (e) hernia formation when repaired with the Surgisis implant and (f) intact abdominal wall defect repaired with the Peri-Guard implant.

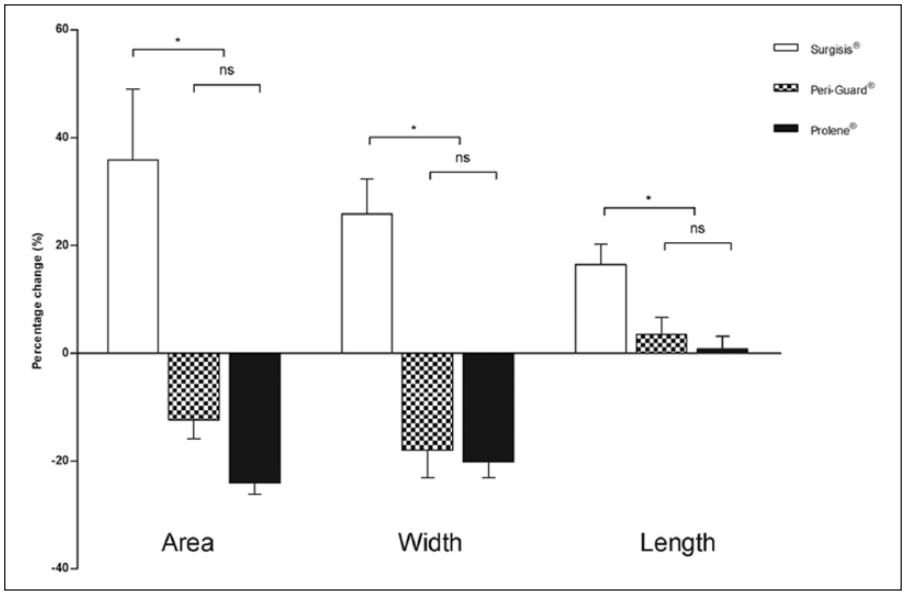

Figure 4. Percentage change of implants in area and dimensions. The Surgisis implant showed an increase in the implant area, while both the Peri-Guard and Prolene implants showed a decrease in the implant area. Surgisis implant showed an increase in the implant width, while both the Peri-Guard and Prolene implants showed a decrease in the implant width. Surgisis, Peri-Guard and Prolene implants all showed an increase in the implant length.
*Statistical significant differences for $p < 0.05$.

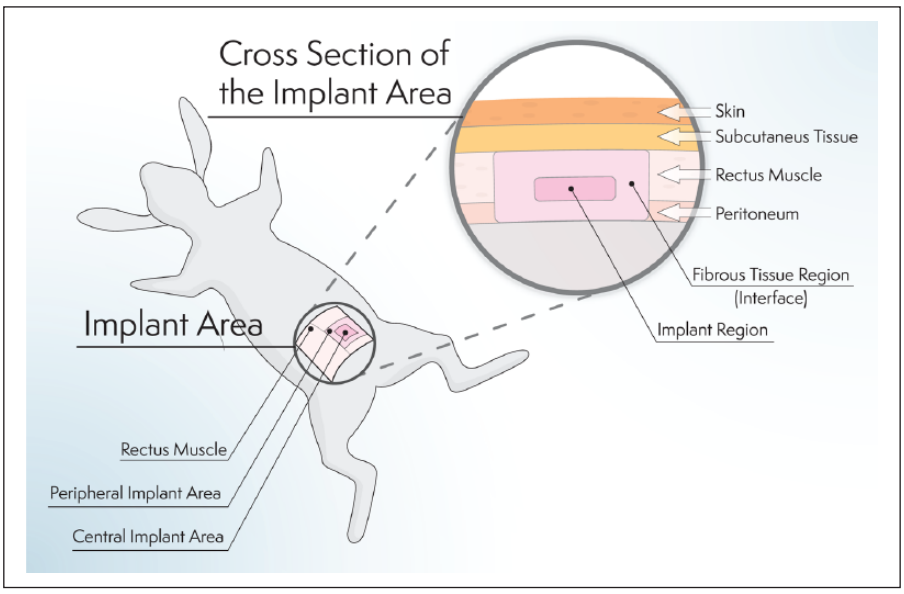

Figure 5. The sampling method employed for histological sectioning and stereological quantification. The implant site was divided into two regions: the implant area and the fibrous tissue region (interface) surrounding the implant. Stereological volume fraction (V_v) estimations of implant, new collagen, fibroblasts, nuclei and blood vessels were used to evaluate tissue composition of implant area.

The implant area of Surgisis had stretched by an average of 35.9%, with a 25.8% increase in width and a 16.5% increase in length observed. All three measurements for Surgisis were statistically higher than for both Peri-Guard and Prolene. Prolene showed the highest percentage shrinkage of 24% of the implant area. However, Peri-Guard showed the smallest percentage shrinkage of just 12.4%.

Histology analysis and stereological quantification

The explanted tissues were further subjected to histological analysis (Figure 5). In the Peri-Guard group, implants were predominantly intact. The dense collagenous implants were not infiltrated by host cells (Figure 6(a)). Blood vessels were observed in the fibrous tissue areas adjacent to the implant surface. The area surrounding the implant consisted of organized collagen and fibroblasts. Inflammatory cells surrounding the implant consisted of lymphocytes, macrophages and foreign body giant cells. There was no host cell or tissue infiltration into the implant area except at the fibrous tissue region immediately adjacent to the host tissue where a higher aggregation of inflammatory cells was observed (Figure 6(b)).

In the Prolene group, polypropylene mesh fibres were surrounded by a layer of inflammatory cells similar to the Peri-Guard group (Figure 6(c)). Adjacent blood vessels were common (Figure 6(d)). There was collagen deposited within the spaces of the polypropylene filaments with fibroblasts frequently observed in between collagen fibres. The layer of collagen appeared disorganized with arrangements in different directions.

In the Surgisis group, implants were almost completely degraded by 56 days. Unlike the Peri-Guard implant, the Surgisis implant was not intact. The degrading fibres were surrounded by inflammatory cells (Figure 6(e)). The Surgisis implant collagen was occasionally observed within macrophages and giant cells indicating their participation in the degradation process (Figure 6(f)). Fibroblasts and collagen deposition were observed adjacent to the degrading implant/degraded implant area. Blood vessels were observed in areas of degradation and areas of collagen deposition.

Changes in the implant area were quantified using stereology based on point counts. The volume fraction (V_v) of the implant, fibroblasts, nuclei and blood vessels were calculated and represented in Figure 7.

With respect to implant and new collagen, it was observed that the Peri-Guard group had the highest V_v of implant (>90%) that was statistically higher than both Prolene and Surgisis. Prolene mesh fibres occupied 33.5% of the implant area by volume fraction 56 days post implantation. In contrast, the V_v of Surgisis was only 3.9% which was statistically lower than Prolene and Peri-Guard. No new collagen formation was observed in the implant area for the Peri-Guard group. Surgisis and Prolene implants showed 35% and 29% of new collagen formed, respectively, as measured by V_v quantification. For cell nuclei, host cells were a major composition of the implant area for both Surgisis and Prolene comprising mainly of lymphocytes and macrophages. Foreign body giant cells were also

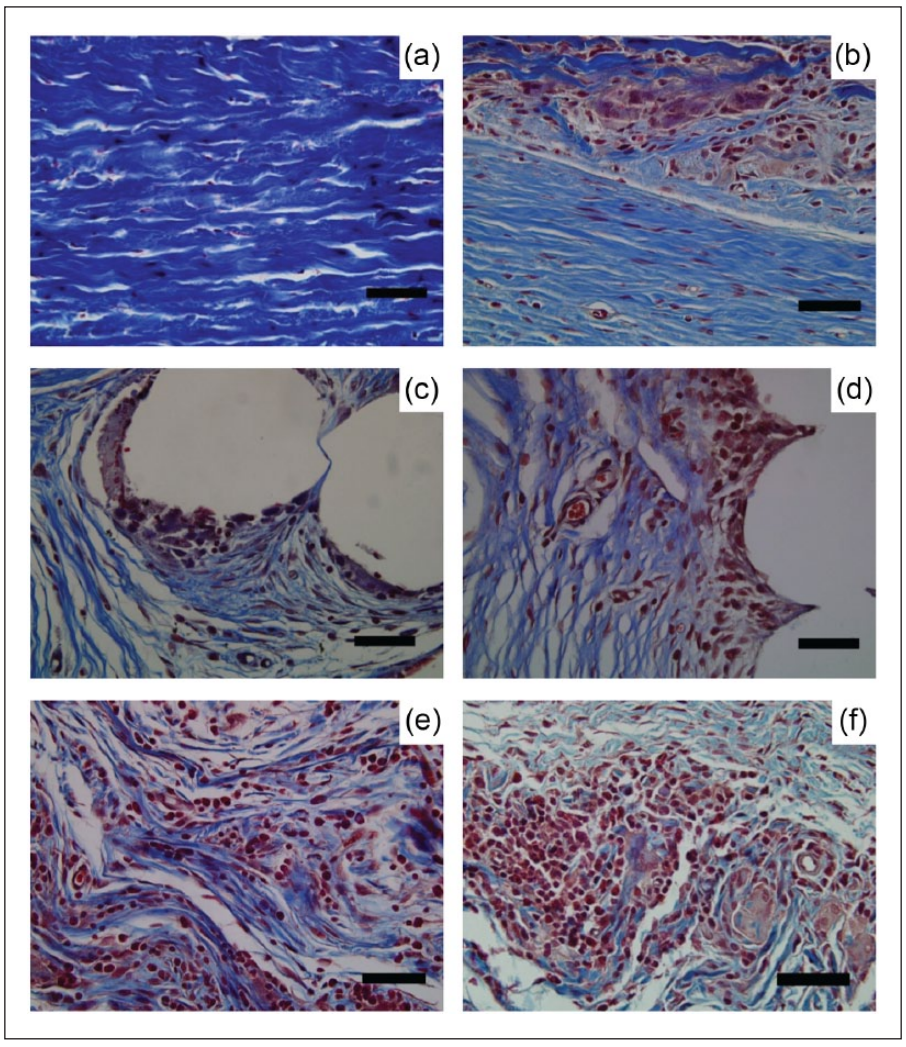

Figure 6. Histology of implant areas and fibrous tissue interface regions of (a, b) Peri-Guard, (c, d) Prolene and (e, f) Surgisis implants, respectively (error bar: 50 μm).

observed adjacent to the implanted material. The V_v of nuclei in Surgisis and Prolene were 16.3% and 8.3%, respectively, which were both statistically significantly higher than Peri-Guard. For fibroblasts, the V_v for Prolene and Surgisis was 11.4% and 9%, respectively, which were both statistically significantly higher than the V_v for Peri-Guard (1.2%). Fibroblasts observed for the Peri-Guard group were sparse in the pericardial tissue. Blood vessels were a minor composition of the implant area as quantified by stereology with a V_v of 2.5% and 1.6% for Prolene and Surgisis, respectively. No blood vessels were detected for Peri-Guard indicating that it is remained an avascular material when placed in vivo.

Discussion

The objective of this study was to design an animal model to investigate the efficacy of surgical meshes for abdominal wall repair. The basis of this model was inspired by the observation in clinical practice that hernia or abdominal weakness developed in patients who had their rectus abdominis muscle harvested for flap surgery.[39–41] There were three unique features of this developed model. First, there was a focus on the evaluation of changes to the implant area (e.g. stretching or shrinkage), which was compared to a control area within the same animal. Second, there was an emphasis on selective anatomical excision of a defined anatomical boundary (unilateral rectus abdominis), rather than a predefined defect size. Finally, we used quantitative stereological methods to analyse histological changes in the implant area.

Three model implants were used to demonstrate the significance of this model. A high-density polypropylene mesh (Prolene) and a thin degradable small intestinal submucosa scaffold (Surgisis) were used to induce contraction and stretching of the implant sites, respectively.[31,32,42,43] It was observed that these two implants behaved as expected. The stretching of Surgisis was statistically significant in

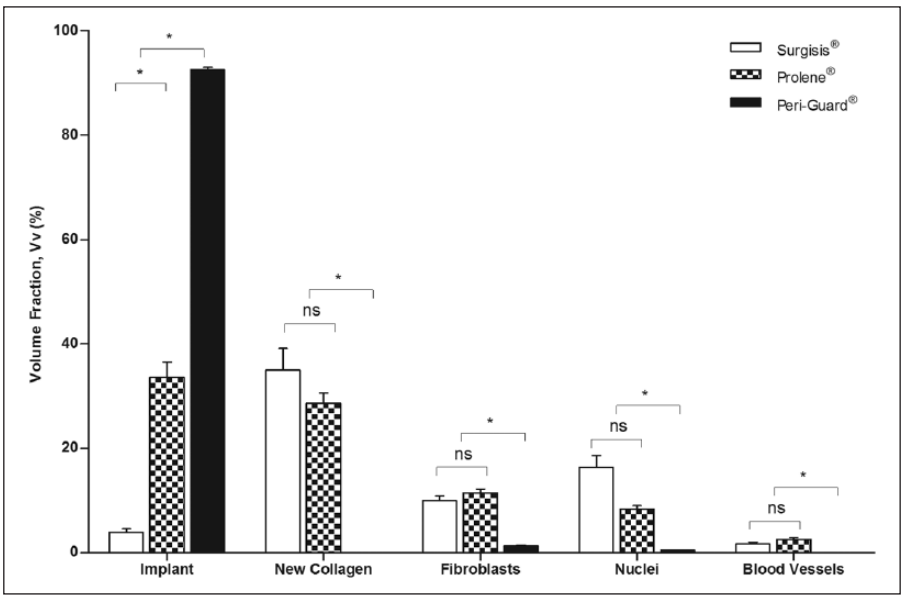

Figure 7. Volume fraction of implant, new collagen, fibroblasts, nuclei and blood vessels for Surgisis, Prolene and Peri-Guard meshes quantified using stereological methods on the implant area.

implant area size, width and length. In contrast, we did not expect the Peri-Guard (glutaraldehyde cross-linked bovine pericardium) implant to show shrinkage of the magnitude observed (12.4%). The hypothesized reasons for this finding includes glutaraldehyde toxicity,[44–46] poor tissue integration and mechanical sheering of the implant/fibrous tissue interface.[47,48] The present in vivo findings are consistent with a previous study that showed glutaraldehyde crosslinking of extracellular matrix resulted in failure of cells to proliferate on these biomaterials in vitro.[49] In addition, since Peri-Guard is a stiff biomaterial that is impermeable to cellular infiltration in vivo, a dense fibrous tissue layer formed around the implanted Peri-Guard. This is indicative of mechanical mismatch and an in vivo response to stabilize the implant site. This role of mechanical irritation on tissue response has been elucidated by Helton et al.[50]

The possibility of 'relative shrinkage' rather than true implant shrinkage was considered as measurements were performed in relation to the contralateral side, which was expected to grow over the experimental time period. Given that the change in length was compared against the excision length of the muscle, an increase would be due to growth with or without stretching. A decrease would be secondary to implant shrinkage, minus growth. The change in width in contrast was determined from the final contralateral muscle width. Therefore, any increase in width greater than the expected growth is interpreted as stretching; while a decrease could either be implant shrinkage (lack of growth or lack of stretching on the test side) or severe hypertrophy on the control side. Taken together, a reduction in length (if final length is shorter than the excision length) was attributed to true implant area shrinkage, while an increase in width (more than the contralateral width) was attributed to true implant stretching. In this study, we observed that there was a 5% increase in length and a corresponding 18% reduction in width for the Peri-Guard implants. This discrepancy can be explained as being either due to true shrinkage or lack of growth/stretching on the implant side (compared to the control muscle width). Another possibility was abnormal hypertrophy on the control side. However, this was not observed, and hence, normal growth of the contralateral side was expected. All considered the effect seen was attributed to Peri-Guard implant shrinkage.

A stereological approach was used for quantitative analysis of histological parameters in the implant area. A quantitative stereological approach was unbiased and powerful to differentiate any changes that may not be easily appreciated utilizing a qualitative or semi-quantitative approach.[37,51] Statistically significant differences in the V_v of the implant, cell nuclei, fibroblasts and blood vessels were observed between the three commercially available scaffolds. Densely cross-linked bovine pericardium Peri-Guard scaffolds showed a high V_v of implant collagen (>90%), while <5% V_v of implant collagen was observed for the degradable Surgisis implant V_v estimation.

The presence of new host collagen, coupled with a higher V_v of cell nuclei and fibroblasts, indicated that the Surgisis implant degradation was almost complete and that remodelling was ongoing. The degradation of Surgisis was not replaced in time by mature host collagen tissue formation. This corresponded to the development of hernia in these animals.

An in vivo model was designed to mimic certain characteristics of the pathology, and hence, there is no ideal or

perfect model. This model has its own limitations. First, our model was based on acute myofascial domain loss in the acute setting, usually due to tumour resection, flap harvest or trauma. Hence, it was not modelled for the more common 'chronic' ventral incisional hernias or groin/inguinal hernias.[52–54] With this in mind, this model does not cover the features of chronic changes associated with delayed fascial failure.[55,56] Nonetheless, we believe that the dimension of the defect created with this model was not inferior to incisional or inguinal hernias. This model can easily be adapted to mimic the presence of a chronic ventral hernia by creating the hernia in the first setting and repair of the defect at a later stage.[57,58] We found that unrepaired defects from a previous pilot study showed that animals implanted with Surgisis developed visible hernias after 3–4 weeks; therefore, this time point should be used for the second surgical intervention. Second, only one defect was created per animal.[59–61] Some investigators had used more than one defect per animal.[33,48,62] We have not done this as it is not known whether one implant will influence the tissue response of a different adjacent implant in the same animal or field. Intuitively, an implant area with an ongoing inflammatory process will affect the tissue response of another implant in the same field. However, randomizing the positions of these implants may reduce any potential effect. Indeed, our model can be adapted for initial screening of potential biomaterials by creating smaller defects on alternating sides of the rectus abdominis. Furthermore, other investigators have performed mesh evaluation without the creation of a defect[63,64] to investigate tissue responses alone.

There have been recent developments in improving the hernia model. DuBay et al.[57] created 'progressive fascial failure' on the abdominal walls of Sprague-Dawley rats by repairing laparotomy wounds using fast absorbing sutures and allowing the fascia repair to fail during the healing period. A similar model was also described by Burcharth et al.[65] based on the idea of a weakly healed abdominal fascia. These techniques were able to model the abnormal wound or fascial healing environment in ventral incisional hernias. The deleterious effects of a weak abdominal wall musculature can be improved following repair in these models.[56,58]

This developed model can be further enhanced for the assessment of other parameters or outcomes. Intraperitoneal placement of surgical meshes has demanded that they induce minimal or no adhesions when implanted. In order to study the strength of adhesions, a model can be created by denuding an area on the abdominal wall and bowel.[66–68] Furthermore, as increasing numbers of biological meshes are used in the contaminated setting,[69,70] animal model with bacteria inoculated into the implant sites[71–73] or caecal puncture (peritonitis model)[74] has been developed to assess the tolerance of implants against infection. Both of these techniques could be incorporated into our model.

To our knowledge, this is the first study to show that biomaterials used to repair the abdominal wall can be compared within the same animal to avoid differences in size and growth. The success of this model relies on two normal recti muscles for comparison. There was no indication that experiments on these animals affected overall growth, whether a reduction or acceleration of growth. Furthermore, a specific muscle is excised, rather than a standardized defect size that is normally reported in the literature. This overcomes the minor differences in defect size excised, as the muscle size is dependent on the anaesthetic level, intra-abdominal pressure, muscle tone and direction of muscle fibres. In this study, we have also shown that stereological techniques can be used successfully to analyse the histological observations to produce quantitative data for comparison.

Conclusion

The presented rabbit model of abdominal wall defect is advantageous for evaluating the in vivo behaviour of biologic surgical meshes as demonstrated here with three commercially available model implants that induced distinct biological responses. Implant area stretching and shrinkage were detected with standard measurements, and histological analysis was performed with quantitative stereological methods to support these findings.

Acknowledgements

The authors acknowledge the editorial assistance of Mr Keith Feerick.

Declaration of conflicting interests

The author(s) declared no potential conflicts of interest with respect to the research, authorship and/or publication of this article.

Funding

This study was financially supported by the Enterprise Ireland (Technology Development Grant). This publication has emanated from research conducted with the financial support of Science Foundation Ireland (SFI) and is co-funded under the European Regional Development Fund under grant no. 13/RC/2073. This study was also supported by the Centre for Microscopy & Imaging funded by NUI Galway and PRTLI, Cycles 4 and 5, National Development Plan 2007–2013.

References

1. Heniford BT, Park A, Ramshaw BJ, et al. Laparoscopic ventral and incisional hernia repair in 407 patients. *J Am Coll Surg* 2000; 190(6): 645–650.
2. Mudge M and Hughes L. Incisional hernia: a 10 year prospective study of incidence and attitudes. *Br J Surg* 1985; 72(1): 70–71.
3. Manninen M, Lavonius M and Perhoniemi V. Results of incisional hernia repair. A retrospective study of 172 unselected hernioplasties. *Eur J Surg* 1991; 157(1): 29–31.

4. Luijendijk RW, Lemmen MH, Hop WC, et al. Incisional hernia recurrence following 'vest-over-pants' or vertical Mayo repair of primary hernias of the midline. *World J Surg* 1997; 21(1): 62–66.
5. Anthony T, Bergen PC, Kim LT, et al. Factors affecting recurrence following incisional herniorrhaphy. *World J Surg* 2000; 24(1): 95–101.
6. Read RC and Yoder G. Recent trends in the management of incisional herniation. *Arch Surg* 1989; 124(4): 485–488.
7. Sugerman HJ, Kellum JM, Reines HD, et al. Greater risk of incisional hernia with morbidly obese than steroid-dependent patients and low recurrence with prefascial polypropylene mesh. *Am J Surg* 1996; 171(1): 80–84.
8. Burger JW, Luijendijk RW, Hop WC, et al. Long-term follow-up of a randomized controlled trial of suture versus mesh repair of incisional hernia. *Ann Surg* 2004; 240(4): 578–585.
9. Read R. Milestones in the history of hernia surgery: prosthetic repair. *Hernia* 2004; 8(1): 8–14.
10. Doran FS, Gibbins RE and Whitehead R. A report on 313 inguinal herniae repaired with nylon nets. *Br J Surg* 1961; 48: 430–434.
11. Read R and Francis C. Usher, herniologist of the twentieth century. *Hernia* 1999; 3(3): 167–171.
12. Usher FC. Hernia repair with knitted polypropylene mesh. *Surg Gynecol Obstet* 1963; 117: 239–240.
13. Usher FC. Hernia repair with Marlex mesh: an analysis of 541 cases. *Arch Surg* 1962; 84: 325–328.
14. Usher FC and Gannon JP. Marlex mesh, a new plastic mesh for replacing tissue defects: I. Experimental studies. *AMA Arch Surg* 1959; 78(1): 131–137.
15. Usher FC, Fries JG, Ochsner JL, et al. Marlex mesh, a new plastic mesh for replacing tissue defects: II. Clinical studies. *AMA Arch Surg* 1959; 78(1): 138–145.
16. Usher FC, Hill JR and Ochsner JL. Hernia repair with Marlex mesh: a comparison of techniques. *Surgery* 1959; 46: 718–724.
17. Usher FC, Ochsner J and Tuttle LL Jr. Use of Marlex mesh in the repair of incisional hernias. *Am Surg* 1958; 24(12): 969–974.
18. Usher FC, Allen JE Jr., Crosthwait RW, et al. Polypropylene monofilament. A new, biologically inert suture for closing contaminated wounds. *JAMA* 1962; 179: 780–782.
19. Jenkins SD, Klamer TW, Parteka JJ, et al. A comparison of prosthetic materials used to repair abdominal wall defects. *Surgery* 1983; 94(2): 392–398.
20. Bauer JJ, Salky BA, Gelernt IM, et al. Repair of large abdominal wall defects with expanded polytetrafluoroethylene (PTFE). *Ann Surg* 1987; 206(6): 765–769.
21. Van der Lei B, Bleichrodt RP, Simmermacher RK, et al. Expanded polytetrafluoroethylene patch for the repair of large abdominal wall defects. *Br J Surg* 1989; 76(8): 803–805.
22. Law NW and Ellis H. Preliminary results for the repair of difficult recurrent inguinal hernias using expanded PTFE patch. *Acta Chir Scand* 1990; 156(9): 609–612.
23. Deysine M. Hernia repair with expanded polytetrafluoroethylene. *Am J Surg* 1992; 163(4): 422–424.
24. Begin GF. Laparoscopic extraperitoneal treatment of inguinal hernias in adults. A series of 200 cases. *Endosc Surg Allied Technol* 1993; 1(4): 204–206.
25. Durden JG and Pemberton LB. Dacron mesh in ventral and inguinal hernias. *Am Surg* 1974; 40(11): 662–665.
26. Hodde J. Naturally occurring scaffolds for soft tissue repair and regeneration. *Tissue Eng* 2002; 8(2): 295–308.
27. Smart NJ, Bryan N and Hunt JA. A scientific evidence for the efficacy of biologic implants for soft tissue reconstruction. *Colorectal Dis* 2012; 14(suppl. 3): 1–6.
28. Judge TW, Parker DM and Dinsmore RC. Abdominal wall hernia repair: a comparison of sepramesh and parietex composite mesh in a rabbit hernia model. *J Am Coll Surg* 2007; 204(2): 276–281.
29. Eberli D, Rodriguez S, Atala A, et al. In vivo evaluation of acellular human dermis for abdominal wall repair. *J Biomed Mater Res A* 2010; 93(4): 1527–1538.
30. Candage R, Jones K, Luchette FA, et al. Use of human acellular dermal matrix for hernia repair: friend or foe? *Surgery* 2008; 144(4): 703–709; discussion 709–711.
31. Shah BC, Tiwari MM, Goede MR, et al. Not all biologics are equal! *Hernia* 2011; 15(2): 165–171.
32. Nahabedian MY. Does AlloDerm stretch? *Plast Reconstr Surg* 2007; 120(5): 1276–1280.
33. Garcia-Urena MA, Vega Ruiz V, Diaz Godoy A, et al. Differences in polypropylene shrinkage depending on mesh position in an experimental study. *Am J Surg* 2007; 193(4): 538–542.
34. Bellon JM, Garcia-Honduvilla N, Rodriguez M, et al. Influence of the structure of new generation prostheses on shrinkage after implant in the abdominal wall. *J Biomed Mater Res B Appl Biomater* 2006; 78(2): 340–346.
35. Welty G, Klinge U, Klosterhalfen B, et al. Functional impairment and complaints following incisional hernia repair with different polypropylene meshes. *Hernia* 2001; 5(3): 142–147.
36. O'Dwyer PJ, Kingsnorth AN, Molloy RG, et al. Randomized clinical trial assessing impact of a lightweight or heavyweight mesh on chronic pain after inguinal hernia repair. *Br J Surg* 2005; 92(2): 166–170.
37. Garcia Y, Breen A, Burugapalli K, et al. Stereological methods to assess tissue response for tissue-engineered scaffolds. *Biomaterials* 2007; 28(2): 175–186.
38. Breen AM, Dockery P, O'Brien T, et al. The use of therapeutic gene eNOS delivered via a fibrin scaffold enhances wound healing in a compromised wound model. *Biomaterials* 2008; 29(21): 3143–3151.
39. Svaerdborg M and Damsgaard TE. Donor-site morbidity after pedicled TRAM breast reconstruction: a comparison of two different types of mesh. *Ann Plast Surg* 2013; 71(5): 476–480.
40. Egeberg A, Rasmussen MK and Sorensen JA. Comparing the donor-site morbidity using DIEP, SIEA or MS-TRAM flaps for breast reconstructive surgery: a meta-analysis. *J Plast Reconstr Aesthet Surg* 2012; 65(11): 1474–1480.
41. Pinell-White XA, Kapadia SM and Losken A. The management of abdominal contour defects following TRAM flap breast reconstruction. *Aesthet Surg J* 2014; 34(2): 264–271.
42. Klinge U, Klosterhalfen B, Muller M, et al. Shrinking of polypropylene mesh in vivo: an experimental study in dogs. *Eur J Surg* 1998; 164(12): 965–969.
43. Silvestre AC, De Mathia GB, Fagundes DJ, et al. Shrinkage evaluation of heavyweight and lightweight polypropylene

meshes in inguinal hernia repair: a randomized controlled trial. *Hernia* 2011; 15(6): 629–634.
44. Van Luyn MJ, Van Wachem PB, Damink LO, et al. Relations between in vitro cytotoxicity and crosslinked dermal sheep collagens. *J Biomed Mater Res* 1992; 26(8): 1091–1110.
45. Bhrany AD, Lien CJ, Beckstead BL, et al. Crosslinking of an oesophagus acellular matrix tissue scaffold. *J Tissue Eng Regen Med* 2008; 2(6): 365–372.
46. Chang Y, Liang HC, Wei HJ, et al. Tissue regeneration patterns in acellular bovine pericardia implanted in a canine model as a vascular patch. *J Biomed Mater Res A* 2004; 69(2): 323–333.
47. Petter-Puchner AH, Fortelny RH, Silic K, et al. Biologic hernia implants in experimental intraperitoneal onlay mesh plasty repair: the impact of proprietary collagen processing methods and fibrin sealant application on tissue integration. *Surg Endosc* 2011; 25(10): 3245–3252.
48. Petter-Puchner AH, Fortelny RH, Walder N, et al. Adverse effects associated with the use of porcine cross-linked collagen implants in an experimental model of incisional hernia repair. *J Surg Res* 2008; 145(1): 105–110.
49. Burugapalli K, Thapasimuttu A, Chan JCY, et al. Scaffold with a natural mesh-like architecture: isolation, structural, and in vitro characterization. *Biomacromolecules* 2007; 8(3): 928–936.
50. Helton KL, Ratner BD and Wisniewski NA. Biomechanics of the sensor-tissue interface-effects of motion, pressure, and design on sensor performance and the foreign body response-part I: theoretical framework. *J Diabetes Sci Technol* 2011; 5(3): 632–646.
51. Henry JA, Burugapalli K, Neuenschwander P, et al. Structural variants of biodegradable polyesterurethane in vivo evoke a cellular and angiogenic response that is dictated by architecture. *Acta Biomater* 2009; 5(1): 29–42.
52. Disa JJ, Goldberg NH, Carlton JM, et al. Restoring abdominal wall integrity in contaminated tissue-deficient wounds using autologous fascia grafts. *Plast Reconstr Surg* 1998; 101(4): 979–986.
53. Leppaniemi A and Tukiainen E. Reconstruction of complex abdominal wall defects. *Scand J Surg* 2013; 102(1): 14–19.
54. Rodriguez ED, Bluebond-Langner R, Silverman RP, et al. Abdominal wall reconstruction following severe loss of domain: the R Adams Cowley Shock Trauma Center algorithm. *Plast Reconstr Surg* 2007; 120(3): 669–680.
55. Voskerician G, Jin J, White MF, et al. Effect of biomaterial design criteria on the performance of surgical meshes for abdominal hernia repair: a pre-clinical evaluation in a chronic rat model. *J Mater Sci Mater Med* 2010; 21(6): 1989–1995.
56. DuBay DA, Choi W, Urbanchek MG, et al. Incisional herniation induces decreased abdominal wall compliance via oblique muscle atrophy and fibrosis. *Ann Surg* 2007; 245(1): 140–146.
57. DuBay DA, Wang X, Adamson B, et al. Progressive fascial wound failure impairs subsequent abdominal wall repairs: a new animal model of incisional hernia formation. *Surgery* 2005; 137(4): 463–471.
58. Culbertson EJ, Xing L, Wen Y, et al. Reversibility of abdominal wall atrophy and fibrosis after primary or mesh herniorrhaphy. *Ann Surg* 2013; 257(1): 142–149.
59. Klosterhalfen B, Klinge U and Schumpelick V. Functional and morphological evaluation of different polypropylene-mesh modifications for abdominal wall repair. *Biomaterials* 1998; 19(24): 2235–2246.
60. Szabo A, Haj M, Waxsman I, et al. Evaluation of seprafilm and amniotic membrane as adhesion prophylaxis in mesh repair of abdominal wall hernia in rats. *Eur Surg Res* 2000; 32(2): 125–128.
61. Bellon JM, Rodriguez M, Garcia-Honduvilla N, et al. Comparing the behavior of different polypropylene meshes (heavy and lightweight) in an experimental model of ventral hernia repair. *J Biomed Mater Res B Appl Biomater* 2009; 89(2): 448–455.
62. Jenkins ED, Melman L, Deeken CR, et al. Biomechanical and histologic evaluation of fenestrated and nonfenestrated biologic mesh in a porcine model of ventral hernia repair. *J Am Coll Surg* 2011; 212(3): 327–339.
63. Novitsky YW, Harrell AG, Cristiano JA, et al. Comparative evaluation of adhesion formation, strength of ingrowth, and textile properties of prosthetic meshes after long-term intra-abdominal implantation in a rabbit. *J Surg Res* 2007; 140(1): 6–11.
64. Matthews BD, Mostafa G, Carbonell AM, et al. Evaluation of adhesion formation and host tissue response to intra-abdominal polytetrafluoroethylene mesh and composite prosthetic mesh. *J Surg Res* 2005; 123(2): 227–234.
65. Burcharth J, Pommergaard HC, Klein M, et al. An experimental animal model for abdominal fascia healing after surgery. *Eur Surg Res* 2013; 51(1–2): 33–40.
66. Harris ES, Morgan RF and Rodeheaver GT. Analysis of the kinetics of peritoneal adhesion formation in the rat and evaluation of potential antiadhesive agents. *Surgery* 1995; 117(6): 663–669.
67. Gonzalez R, Rodeheaver GT, Moody DL, et al. Resistance to adhesion formation: a comparative study of treated and untreated mesh products placed in the abdominal cavity. *Hernia* 2004; 8(3): 213–219.
68. Dinsmore RC, Calton WC Jr., Harvey SB, et al. Prevention of adhesions to polypropylene mesh in a traumatized bowel model. *J Am Coll Surg* 2000; 191(2): 131–136.
69. Pinell-White XA, Gruszynski M and Losken A. Ventral hernia repair after bowel surgery: does gastrointestinal contamination matter in the era of biologic mesh? *Ann Plast Surg* 2014; 72(6): S150–S152.
70. Sbitany H, Kwon E, Chern H, et al. Outcomes analysis of biologic mesh use for abdominal wall reconstruction in clean-contaminated and contaminated ventral hernia repair. *Ann Plast Surg* 2013; 75: 201–204.
71. Harth KC, Broome AM, Jacobs MR, et al. Bacterial clearance of biologic grafts used in hernia repair: an experimental study. *Surg Endosc* 2011; 25(7): 2224–2229.
72. Harth KC, Blatnik JA, Anderson JM, et al. Effect of surgical wound classification on biologic graft performance in complex hernia repair: an experimental study. *Surgery* 2013; 153(4): 481–492.
73. Milburn ML, Holton LH, Chung TL, et al. Acellular dermal matrix compared with synthetic implant material for repair of ventral hernia in the setting of peri-operative Staphylococcus aureus implant contamination: a rabbit model. *Surg Infect (Larchmt)* 2008; 9(4): 433–442.
74. Deerenberg EB, Mulder IM, Grotenhuis N, et al. Experimental study on synthetic and biological mesh implantation in a contaminated environment. *Br J Surg* 2012; 99(12): 1734–1741.